

## SUPPLEMENTARY INFORMATION

### **Adaptation of the protein misfolding cyclic amplification (PMCA) technique for the screening of anti-prion compounds.**

Katherine Do<sup>1</sup>, Rebeca Benavente<sup>1</sup>, Celso S. G. Catumbela<sup>1</sup>, Uffaf Khan<sup>1</sup>, Carlos Kramm<sup>1</sup>,  
Claudio Soto<sup>1</sup> and Rodrigo Morales<sup>1,2\*</sup>.

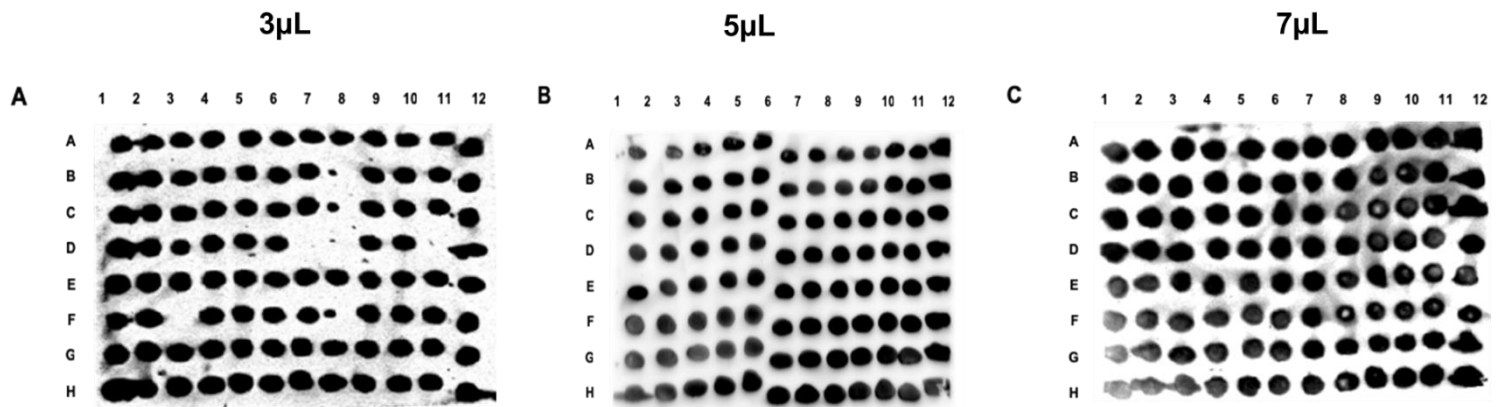
<sup>1</sup>Department of Neurology, The University of Texas Health Science Center at Houston. Houston, TX 77030. United States of America.

<sup>2</sup>Centro Integrativo de Biología y Química Aplicada (CIBQA). Universidad Bernardo O'Higgins. Santiago. Chile.

\*To whom correspondence should be addressed: [Rodrigo.MoralesLoyola@uth.tmc.edu](mailto:Rodrigo.MoralesLoyola@uth.tmc.edu)

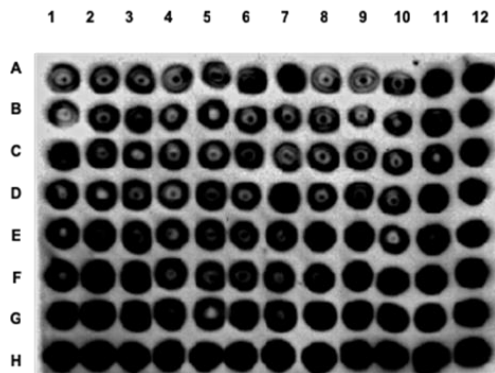
**Supplementary Table 1. Previously reported active concentrations for some of the anti-prion and anti-amyloid compounds used in this study.** The results provided in this table are based in previous reports (as referenced) and used in cell culture models of prion replication (or other amyloids), aggregation assays or bioassays.

<b>Compound</b>	<b>Literature-reported active concentrations</b>
<i>Tannic Acid</i>	0.1 $\mu\text{M}^1$
<i>Astemizole</i>	0.5-1 $\mu\text{M}^1$
<i>Congo Red</i>	1-100 $\mu\text{M}^2$
<i>Curcumin</i>	10 $\mu\text{M}^1$
<i>Quinacrine dihydrochloride</i>	0.1-0.5 $\mu\text{M}^1$
<i>Imatinib</i>	10 $\mu\text{M}^3$
<i>Reservatrol</i>	1-200 $\mu\text{M}^4$
<i>Tetracycline HCl</i>	100 $\mu\text{M}$ - 1 $\mu\text{M}^5$
<i>Thioflavin T</i>	122 $\mu\text{M}$ (For Amyloid $\beta$ ) <sup>6</sup>
<i>Tetrandrone</i>	1-10 $\mu\text{M}^1$
<i>Azure A</i>	0.108 $\mu\text{M}$ (For tau) <sup>7</sup>
<i>Azure B</i>	2.5 $\mu\text{M}$ (For Amyloid $\beta$ ) <sup>8</sup>
<i>Azure C</i>	0.09 $\mu\text{M}$ (For Amyloid $\beta$ ) <sup>6</sup>
<i>Quinacrine mustard</i>	2.051 mM (For Amyloid $\beta$ ) <sup>6</sup>
<i>Rhodanine</i>	309 $\mu\text{M}$ (For Amyloid $\beta$ ) <sup>6</sup>
<i>Thionine acetate</i>	0.098 $\mu\text{M}$ (For Tau) <sup>7</sup>



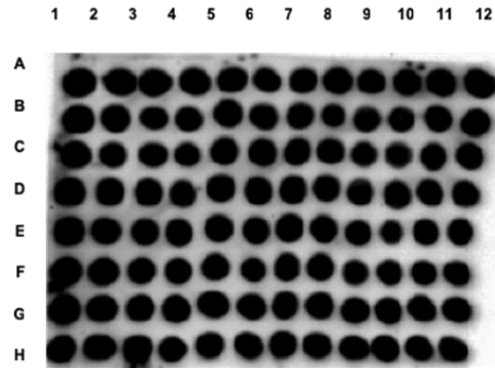
**Supplementary Figure 1. Effect of sample volume in the dot assay.** Different volumes of sample including 3 (A), 5 (B) and 7 (C) µL were loaded into the nitrocellulose membrane as described in Methods.

A



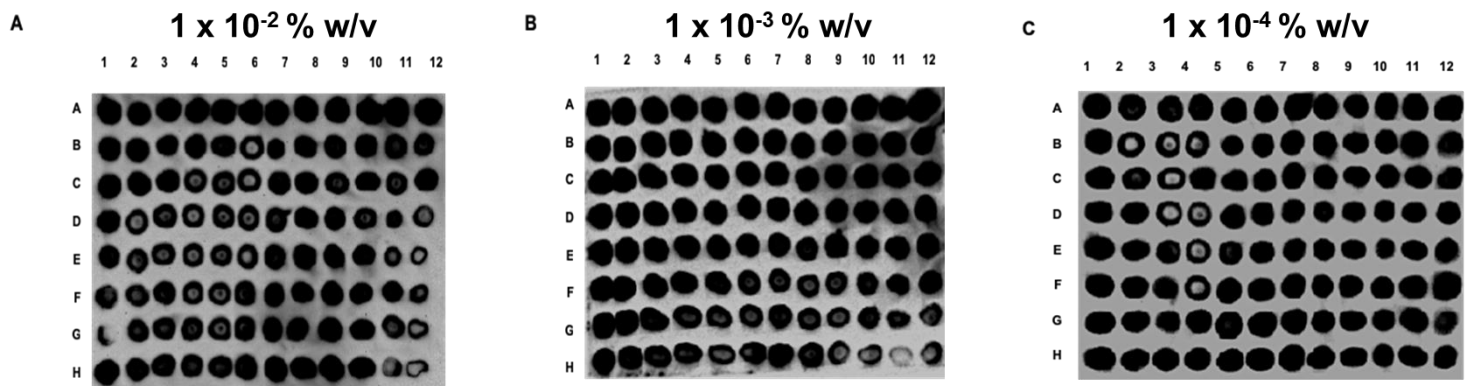
24 hours

B



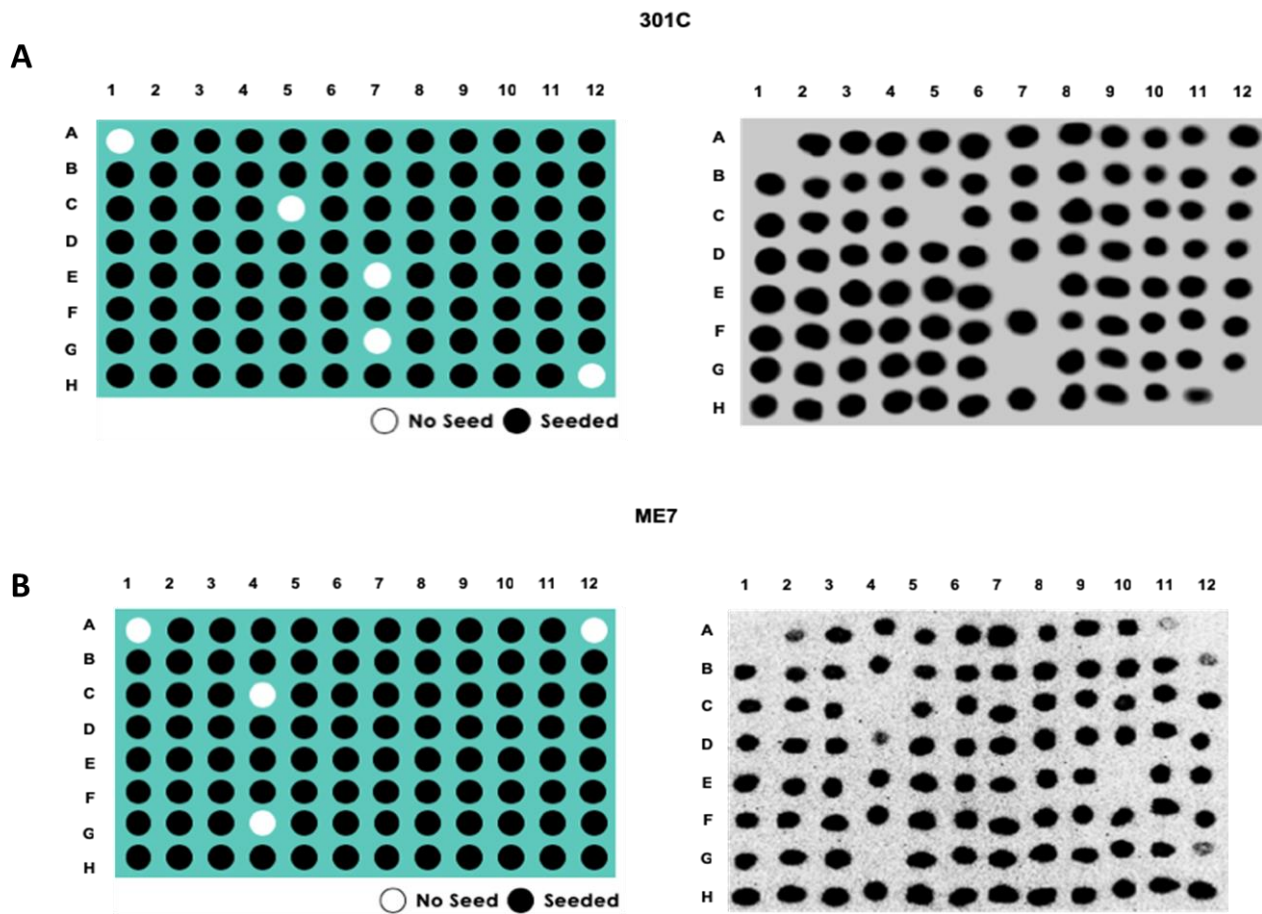
48 hours

**Supplementary Figure 2. Effect of the number of incubation/sonication cycles in PMCA replication using 96 well plates.** Different incubation/sonication cycles extending for a total of 24 (**A**) or 78 (**B**) hours were tested using RML prions. All samples were treated with PK before loading them in the nitrocellulose membrane as described in Methods.

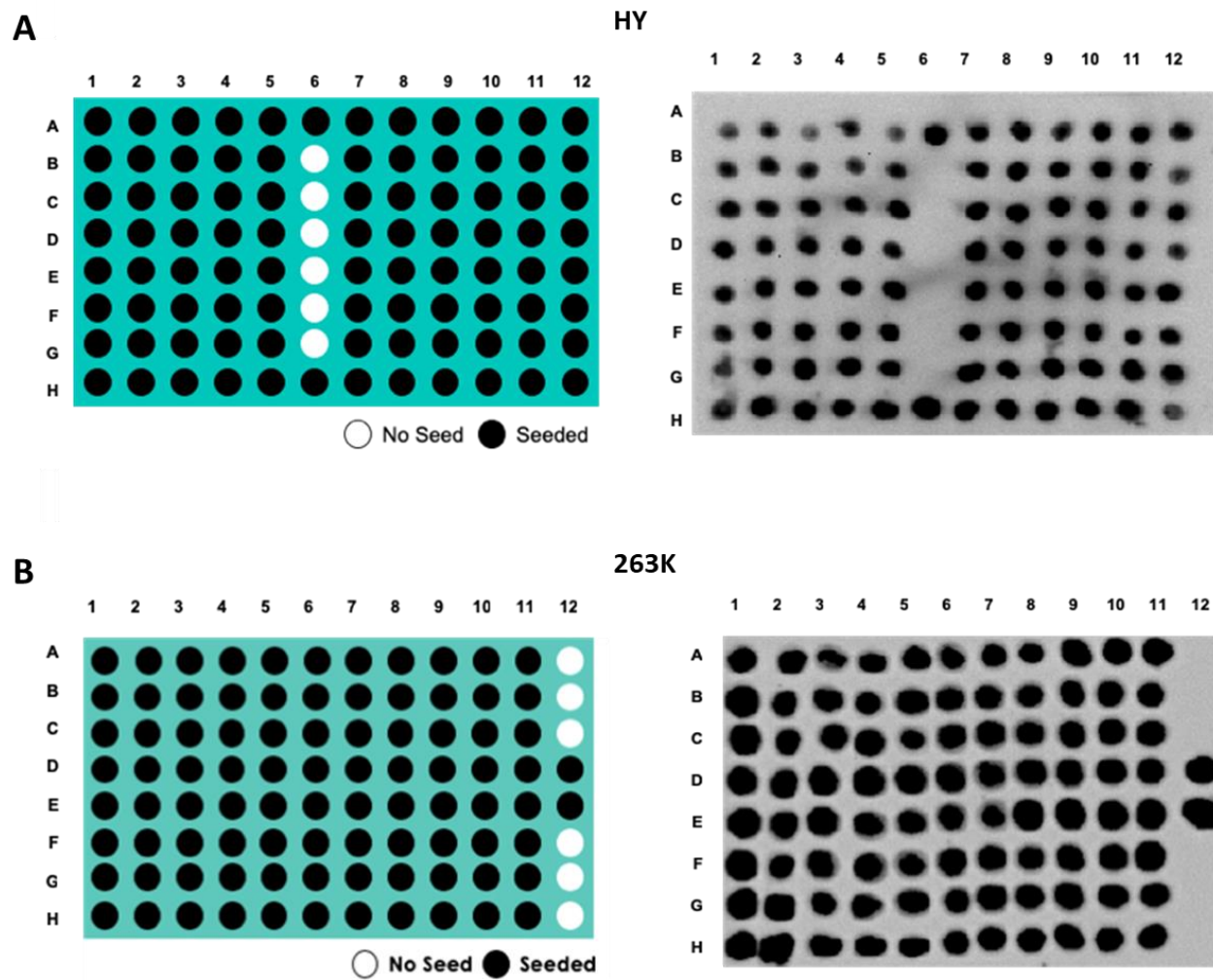


**Supplementary Figure 3. Effects of varying PrP<sup>Sc</sup> concentrations in the 96wp-PMCA assay.**

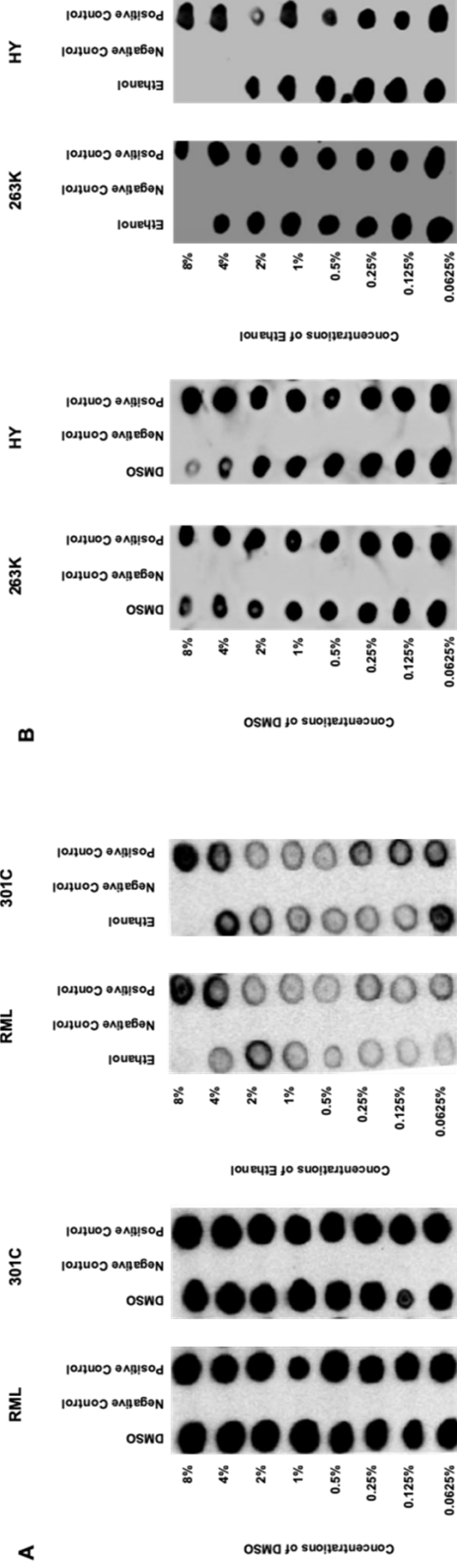
To explore the minimum concentration of prions allowing for uniform detection across a 96 well plate, several dilutions of a brain extract containing RML prions were used. These dilutions were as follows:  $10^{-2}$  (**A**),  $10^{-3}$  (**B**), and  $10^{-4}$  (**C**). All samples were treated with PK before been loaded in the nitrocellulose membrane as described in Methods.



**Supplementary Figure 4. Representative panels of optimized 96wp-PMCA assays for 301C and ME7 mouse prion strains.** *In vitro* replication of 301C (A) or ME7 (B) prions. Left panels explain how seeded (black circles) and unseeded (white circles) reactions were positioned across the 96 well plate. Right panels demonstrate actual results. All samples shown in this experiment were PK treated before been loaded in the nitrocellulose membrane as described in Methods.

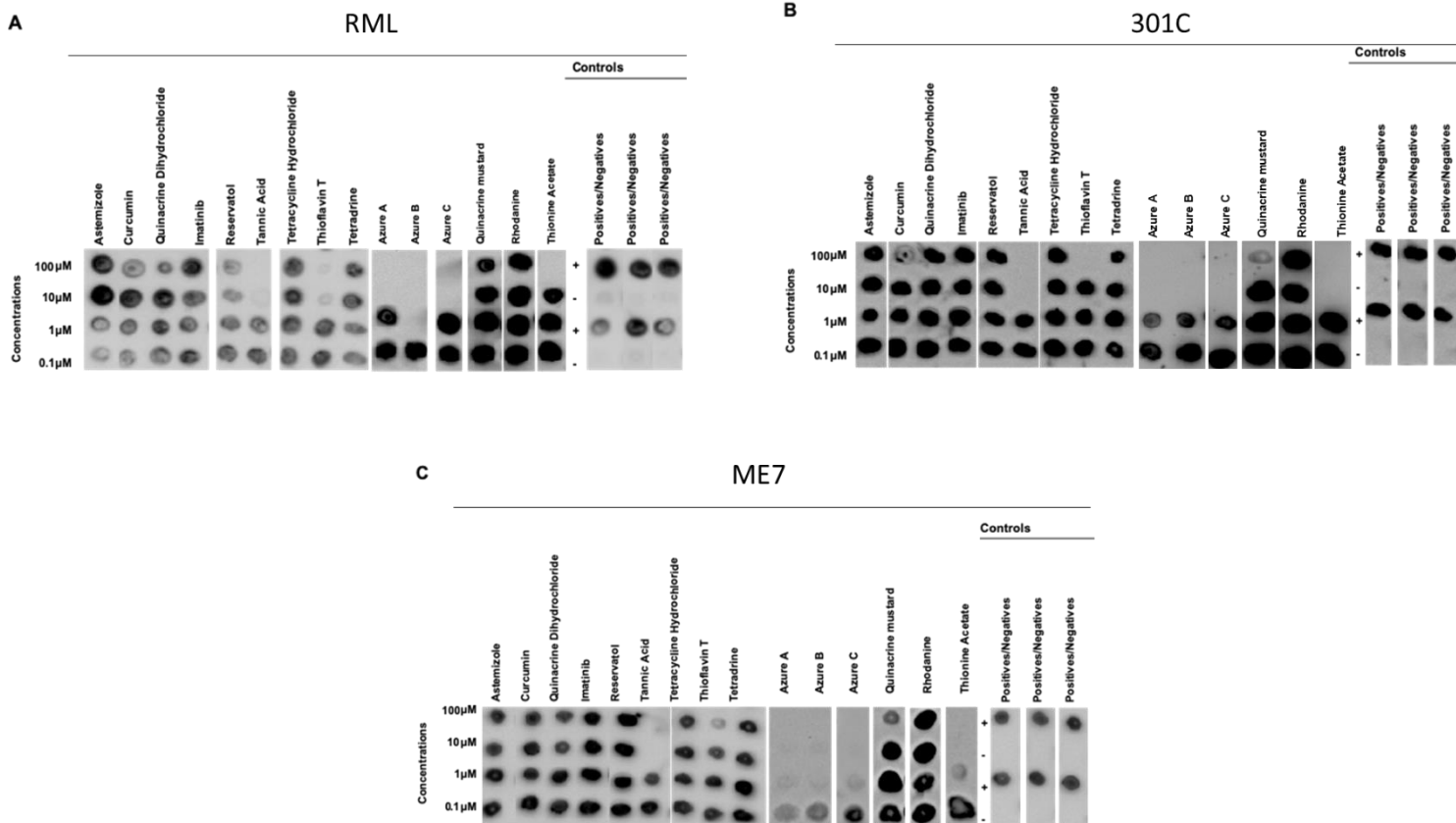


**Supplementary Figure 5. Representative panels of optimized 96wp-PMCA assays for HY and 263K mouse prion strains.** *In vitro* replication of HY (A) or 263K (B) prions. Left panels explain how seeded (black circles) and unseeded (white circles) reactions were positioned across the 96 well plate. Right panels demonstrate actual results. All samples shown in this experiment were PK treated before visualized in dot blots, as described in Methods.

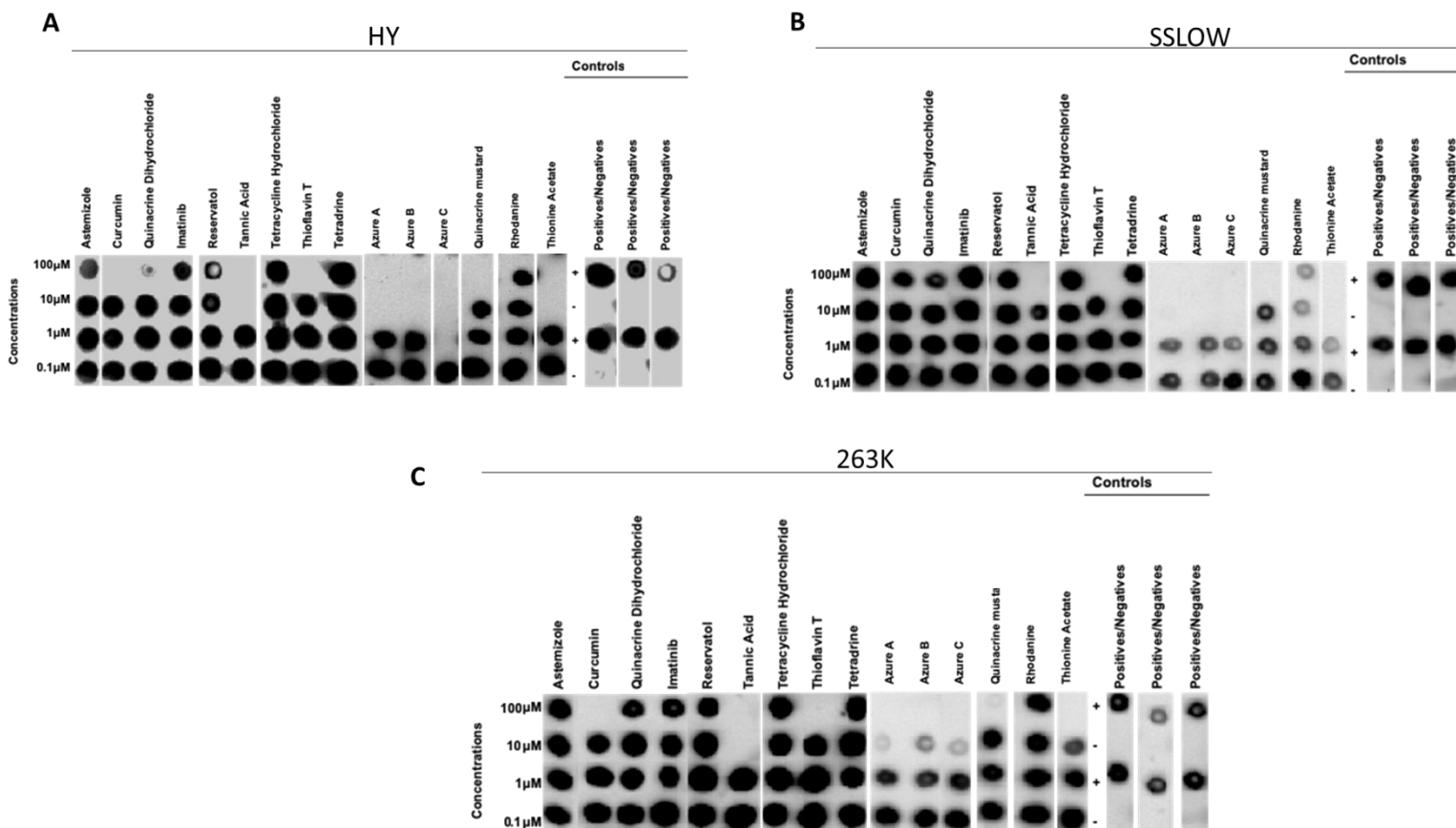


**Supplementary figure 6: Effect of different solvents in 96wp-PMCA.** Serial dilutions of either DMSO (left panels) or EtOH (right panels) (ranging from 8 to 0.0625%) were tested in two different mouse (RML and 301C **(A)**) and Syrian hamster (263K and HY **(B)**) prion strains.

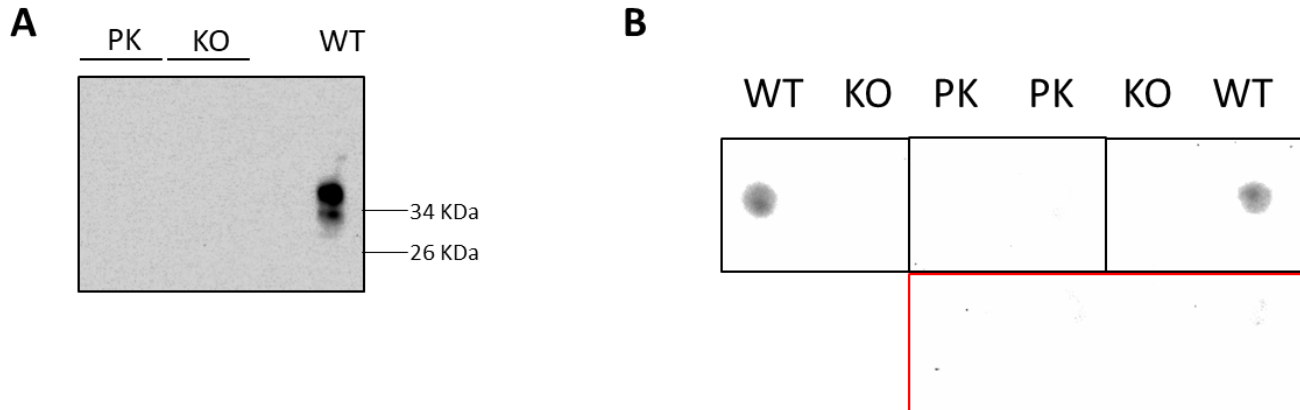




**Supplementary Figure 7. Specific activity of small molecules of known anti-prion and anti-amyloid activity in mouse prion strains (dissolved in EtOH).** Fifteen small molecules with proven anti-prion or anti-amyloid activity (dissolved in EtOH) were tested at four different concentrations for their anti-prion activities against the RML (**A**), 301C (**B**) and ME7 (**C**) prion strains using the 96wp-PMCA. Each molecule was tested in concentrations ranging from 0.1 to 100  $\mu$ M. Controls for solvent representative for all strains, positive samples and negative samples without compounds were included to monitor the assay. Dot blots were modified for labeling. The panels shown in this figure are representative from three independent assays. Congo Red (previously tested in the DMSO condition) was not included in this analysis.



**Supplementary Figure 8. Specific activity of small molecules of known anti-prion and anti-amyloid activity in Syrian hamster prion strains (dissolved in EtOH).** Fifteen small molecules with proven anti-prion or anti-amyloid activity (dissolved in EtOH) were tested at four different concentrations for their anti-prion activities against the HY (**A**), SSLOW (**B**) and 263K (**C**) prion strains using the 96wp-PMCA. Each molecule was tested in concentrations ranging from 100  $\mu$ M to 0.1  $\mu$ M. Controls for solvent representative for all strains, positive samples and negative samples without compounds were included to monitor the assay. Dot blots were modified for labeling. The panels shown in this figure are representative from three independent assays. Congo Red (previously tested in the DMSO condition) was not included in this analysis.



**Supplementary Figure 9. Effect of PrP<sup>C</sup> removal in the 96wp-PMCA reactions. A)** Western blot of the different substrates used in this experiment, including a PK-treated (PK) wild-type mouse brain extract, and a brain homogenate from a PrP<sup>C</sup> knock out (KO) mouse. A brain of an untreated wild type mouse (WT) was used as control. Numbers at the right represent molecular weight markers. **B)** 96-wp PMCA products were visualized by dot blots using the different substrates described in (A). The red square denotes four unseeded reactions using the WT substrate (negative controls).

## REFERENCES

1. Kocisko, D.A., Baron, G.S., Rubenstein, R., Chen, J., Kuizon, S., and Caughey, B. (2003). New Inhibitors of Scrapie-Associated Prion Protein Formation in a Library of 2,000 Drugs and Natural Products. *J Virol* 77, 10288–10294. 10.1128/jvi.77.19.10288-10294.2003.
2. Rudyk, H., Birkett, C.R., Hennion, R.M., Gilbert, I.H., Hope, J., and Vasiljevic, S. (2000). Screening Congo Red and its analogues for their ability to prevent the formation of PrP-res in scrapie-infected cells. *Journal of General Virology* 81, 1155–1164. 10.1099/0022-1317-81-4-1155.
3. Yun, S.-W., Ertmer, A., Flechsig, E., Gilch, S., Riederer, P., Gerlach, M., Schätzl, H.M., and Klein, M.A. (2007). The tyrosine kinase inhibitor imatinib mesylate delays prion neuroinvasion by inhibiting prion propagation in the periphery. *J Neurovirol* 13, 328–337. 10.1080/13550280701361516.
4. Wang, J., Zhang, B.-Y., Zhang, J., Xiao, K., Chen, L.-N., Wang, H., Sun, J., Shi, Q., and Dong, X.-P. (2016). Treatment of SMB-S15 Cells with Resveratrol Efficiently Removes the PrPSc Accumulation In Vitro and Prion Infectivity In Vivo. *Mol Neurobiol* 53, 5367–5376. 10.1007/s12035-015-9464-z.
5. Forloni, G., Iussich, S., Awan, T., Colombo, L., Angeretti, N., Girola, L., Bertani, I., Poli, G., Caramelli, M., Grazia Bruzzone, M., et al. (2002). Tetracyclines affect prion infectivity. *Proceedings of the National Academy of Sciences* 99, 10849–10854. 10.1073/pnas.162195499.
6. Necula, M., Kaye, R., Milton, S., and Glabe, C.G. (2007). Small Molecule Inhibitors of Aggregation Indicate That Amyloid  $\beta$  Oligomerization and Fibrillization Pathways Are Independent and Distinct. *Journal of Biological Chemistry* 282, 10311–10324. 10.1074/jbc.M608207200.
7. Sonawane, S.K., Chidambaram, H., Boral, D., Gorantla, N.V., Balmik, A.A., Dangi, A., Ramasamy, S., Marelli, U.K., and Chinnathambi, S. (2020). EGCG impedes human Tau aggregation and interacts with Tau. *Sci Rep* 10, 12579. 10.1038/s41598-020-69429-6.
8. Biberoglu, K., Yuksel, M., and Tacal, O. (2019). Azure B affects amyloid precursor protein metabolism in PS70 cells. *Chem Biol Interact* 299, 88–93. 10.1016/j.cbi.2018.11.023.